Behavioural Brain Research 433 (2022) 113999

Contents lists available at ScienceDirect

Behavioural Brain Research

journal homepage: www.elsevier.com/locate/bbr

Resting-state neural signal variability in women with depressive disorders

Sally Pessin [a], Erin C. Walsh [b], Roxanne M. Hoks [c], Rasmus M. Birn [d], Heather C. Abercrombie [c], Carissa L. Philippi [a,*]

[a] Department of Psychological Sciences, University of Missouri-St. Louis, 1 University Blvd., St. Louis, MO 63121, USA
[b] Department of Psychiatry, University of North Carolina at Chapel Hill School of Medicine, CB# 7167, Chapel Hill, NC 27599, USA
[c] Center for Healthy Minds, University of Wisconsin-Madison, 625W. Washington Ave., Madison, WI 53703, USA
[d] Department of Psychiatry, University of Wisconsin-Madison, 6001 Research Park Blvd., Madison, WI 53719, USA

ARTICLE INFO

Keywords:
Depression
Neural signal variability
BOLD variability
Default mode network
Salience network
Frontoparietal network
Machine learning

ABSTRACT

Aberrant activity and connectivity in default mode (DMN), frontoparietal (FPN), and salience (SN) network regions is well-documented in depression. Recent neuroimaging research suggests that altered variability in the blood oxygen level-dependent (BOLD) signal may disrupt normal network integration and be an important novel predictor of psychopathology. However, no studies have yet determined the relationship between resting-state BOLD signal variability and depressive disorders nor applied BOLD signal variability features to the classification of depression history using machine learning (ML). We collected resting-state fMRI data for 79 women with different depression histories: no history, past history, and current depressive disorder. We tested voxelwise differences in BOLD signal variability related to depression group and severity. We also investigated whether BOLD signal variability of DMN, FPN, and SN regions could predict depression history group using a supervised random forest ML model. Results indicated that individuals with any history of depression had significantly decreased BOLD signal variability in the left and right cerebellum and right parietal cortex (p_{FWE} <0.05). Furthermore, greater depression severity was also associated with reduced BOLD signal variability in the cerebellum. A random forest model classified participant depression history with 74% accuracy, with the ventral anterior cingulate cortex of the DMN as the most important variable in the model. These findings provide novel support for resting-state BOLD signal variability as a marker of neural dysfunction in depression and implicate decreased neural signal variability in the pathophysiology of depression.

1. Introduction

Depression is a debilitating psychiatric condition characterized by consistent depressed mood and fatigue, feelings of worthlessness, and an inability to feel pleasure [1]. Depressive disorders are the leading cause of disability, affecting more than 320 million of the global population [2,3]. There is also a relatively high rate of recurrence in depression, with subsequent depressive episodes further exacerbating the negative personal and societal consequences associated with the disorder [4 for review]. Due to its prevalence and risk for recurrence, it is critical to explore the neurobiological aspects of depressive disorders as neural mechanisms may inform personalized medicine and provide biomarkers for early intervention and treatment.

Several neurobiological models suggest that dysfunction of large-scale cortical and subcortical networks may underlie the affective and cognitive symptoms of depression, including the default mode network (DMN), the frontoparietal network (FPN), and the salience network (SN) [5–9]. Neuroimaging studies have frequently reported heightened activity and connectivity of the DMN, consisting of the medial prefrontal cortex (mPFC), posterior cingulate cortex (PCC), retrosplenial cortex, and the inferior parietal lobule (IPL) in depression [10–12]. For example, using task-based and resting-state functional neuroimaging, elevated activity and connectivity within the DMN has been associated with greater depressive symptoms and negative self-reference in depression [11,13–17]. In particular, abnormal activity and connectivity with the mPFC and subgenual anterior cingulate cortex may contribute to sad mood, rumination, and vegetative symptoms of major depressive disorder [5–7,9,10]. Further, disrupted connectivity between the DMN and other networks has also been reported in depression. It has been argued that since DMN activity is primarily associated with internal and self-referential thoughts, this may come at a cost to other networks concerned with externally directed attention and cognition,

* Correspondence to: 1 University Boulevard, St. Louis, MO 63121, USA.
E-mail address: philippic@umsl.edu (C.L. Philippi).

https://doi.org/10.1016/j.bbr.2022.113999
Received 24 February 2022; Received in revised form 15 June 2022; Accepted 5 July 2022
Available online 8 July 2022

such as FPN and SN [9,11]. For example, the FPN, which comprises the dorsolateral prefrontal cortex (dlPFC) and intraparietal sulcus (IPS), has shown lower inverse correlations with the DMN in individuals with depression in comparison to healthy individuals [9,18]. Altered connectivity in depression was also found between the DMN and the amygdala and anterior insula of the SN [18–20]. Moreover, reduced connectivity among FPN and SN regions has been associated with depression [20–23]. Altogether, prior work indicates that there is a distinct association between depression and large-scale functional network disruption. However, most resting-state neuroimaging studies to date have examined the DMN, FPN, and SN mean connectivity of the BOLD signal, so it remains unclear how higher-order measures of neural activity (i.e., variability) in these networks relate to depression.

As an alternative to fMRI measures of activity and connectivity as described above that utilize the mean BOLD signal, recent studies have explored BOLD signal variability as a novel tool for examining individual differences in resting-state activity. Researchers have proposed that a sufficient degree of neural variability may be required for an "optimal" level for functioning and also promote network integration [24,25]. In support of this hypothesis, an optimal amount of variability was associated with better communication between network regions and overall better functioning systems [24]. Further research on stochastic resonance supports this notion, demonstrating that the addition of noise (i.e., variability) is necessary to detect some weak resting-state signals, and too much or too little variability may hinder neural synchronization [26,27]. Similarly, Easson and McIntosh [28] suggested a moderate amount of variability is required for neural systems to switch from state to state, and too little variability may impede adaptation to external information in new environments. Theoretically, the ability of network regions to optimally respond to new stimuli also reflects Bayesian probabilities where optimization occurs through conditional probabilities before and after information integration. That is, if the signal remained constant, there would be no new information to analyze and, therefore, no range of responses from which to select. For this reason, neural variability can be considered the neurobiological mechanism of adaptability [29,30].

Measuring variability in fMRI data has been operationalized as the standard deviation (SD) or fractional SD (fSD) of BOLD signal, the mean squared successive differences of BOLD signal, amplitude of low frequency fluctuations (ALFF), and fractional ALFF (fALFF). These measures of neural variability have been well characterized in relation to age, with largely decreased variability across development [26,27,31–33]. Subsequent studies have investigated these measures in a variety of psychiatric and neurodegenerative disorders, such as mood and anxiety disorders [34–37], attention-deficit hyperactivity disorder [38], autism [28], Alzheimer's disease [39,40], and in clinical subtypes and temperament relevant to depression [37,41–43]. For example, in a task-based study where participants passively viewed emotionally salient film clips, individuals with the melancholic subtype of depression exhibited decreased BOLD signal variability within the ventral mPFC of the DMN in comparison to healthy controls [41]. In Bipolar Disorder (BD), a resting-state study revealed higher BOLD signal variability in DMN regions paired with lower variability in sensorimotor network (SMN) regions in a depressed subgroup of BD [37]. Analogous patterns of altered between-network variability during resting-state scans were found in a similar sample of depressed individuals with BD, with increased variability in the ACC, ventral mPFC, orbitofrontal cortex, pallidum, and brainstem combined with decreased variability in the occipital cortex, cerebellum, cingulate gyrus, and medial limbic regions [42]. Depressive temperament has also been explored in relation to BOLD signal variability, where individuals with depressive temperament exhibited significantly decreased signal variability in SMN regions [43]. It is clear from previous research there is altered variability in relation to depressive symptoms. However, there is little literature explicitly examining BOLD signal variability as a function of unipolar depression history and severity.

In pursuit of advancing current knowledge on the association between BOLD signal variability and depression, it is also important to consider the promising opportunities offered by machine learning (ML). ML methods are increasingly being used for their ability to create computer-aided statistical models from low- and high-dimensional data, such as structural and functional MRI data [44,45]. In fact, the potential of these algorithms to classify patients into separate psychiatric conditions and treatment responses has been explored using behavioral, genetic, and neurobiological data [46,47]. In relation to depression, several studies have used ML to classify individuals based on clinical symptom measures or structural or functional imaging methods. For example, Haslam and Beck [48] initially demonstrated the potential of ML algorithms for diagnostic classification using Beck Depression Inventory (BDI) item scores to classify syndromal subtypes of depression. Contemporary applications have used ML algorithms with quantitative brain imaging measurements to predict diagnostic groups and treatment responses and outcomes [46]. For instance, average structural and functional measures from fMRI, electroencephalograms (EEG), and diffusion tensor imaging (DTI) have been utilized in both supervised and unsupervised models as features to classify individuals by psychiatric symptoms and diagnosis in relation to depression [49–55]. In a study comparing ML methods in late-life depression classification, a supervised alternating decision trees method outperformed other ML methods (AUC = 87.27%) when using resting-state fMRI ROIs selected from the DMN [51]. Wade et al. [44] utilized an RF classification method and identified two morphological descriptors in MRI anatomical images that differentiated individuals with depression from healthy controls. Similarly, an RF model achieved 75% accuracy when applied in the classification of suicidal behavior through 47 rsFC features [49]. Through unsupervised maximum margin clustering, Zeng and colleagues [55] established the resting-state functional connections between the subgenual and pregenual ACC provided 92.5% and 84.9% accuracy, respectively, in categorizing depressed patients from healthy controls. Few studies have examined BOLD signal variability as a feature in the ML classification of depression, let alone as a feature in any ML algorithm. That being said, Gaut et al. [56] achieved 84% accuracy using BOLD signal variability to predict the identity of a healthy subject performing a task and the type of task performed within scan sessions. Moreover, they obtained 63% accuracy when assessing the predictive ability of BOLD signal variability for subject identity at rest and found that BOLD signal variability, in general, was reduced during rest in comparison to during tasks. From these findings, it is evident ML algorithms present a unique opportunity to combine behavioral and functional neuroimaging data in predictive modeling. Furthermore, RF classification appears promising in the classification of depression diagnosis and history. However, it remains unclear how modeling higher-order measures of neural activity (e.g., BOLD signal variability) would perform and affect the predictive ability of diagnostic classification models in depression.

To our knowledge, no studies have yet investigated resting-state BOLD signal variability in relation to varying unipolar depression histories and severities. The current study aimed to investigate resting-state BOLD signal variability in both global brain activity and topographical patterns in relation to depression history and severity. First, we hypothesized that currently depressed individuals would show lower BOLD signal variability, in particular in regions of the DMN, than individuals with a past depression history and individuals with no history of depression. Second, we hypothesized that there would be a negative relationship between depression symptom severity and voxel-wise resting-state BOLD signal variability, particularly within regions of the DMN. We also used a supervised random forest ML model to determine whether BOLD signal variability in regions of the DMN, FPN, and SN could be used to predict depression history group membership.

2. Material and methods

2.1. Participants and procedures

Eighty-five women were recruited as part of a larger NIH funded study investigating the effects of cortisol on cognitive and neural function in depression [57–59]. In the larger study, structured interviews were conducted to clinically characterize participants, then participants completed two fMRI scans typically one week apart: one placebo scan and one hydrocortisone scan. An hour prior to each scan, participants received a pill containing either a placebo or 20 mg hydrocortisone. Drug administration was double-blind and randomized across the two fMRI sessions. Data reported in the current study were taken from the placebo day fMRI scan.

For the present study, full neuroimaging data available were available for 79 participants, with ages ranging from 18 to 45 (M_{age} = 27.6, SD_{age} = 7.0). Participants were categorized into three separate groups based on their depression history and severity: (*i*) no history of depression (n = 30; NoDep); (*ii*) history of depression, but not currently depressed (n = 15; PastDep); and (*iii*) currently depressed, meeting the diagnostic criteria for a DSM-5 Depressive Disorder (n = 34; CurrentDep). To further examine the influence of depression history, participants were also categorized with a two-level depression history classification: (*i*) no history of depression (n = 30; NoDep); (*ii*) any history of depression (n = 49; DepHist). With the exception of one subject who received a diagnosis of Social Phobia in partial remission during the SCID interview, participants in the NoDep group did not present with any other psychiatric conditions. See Table 1 for additional participant information.

All participants were screened for psychopathology using the Structured Clinical Interview for the DSM-IV, modified to assess DSM-5 criteria [SCID-I/P for DSM-IV-TR, 60]. Exclusion criteria were as follows: lifetime history of psychosis or mania; current substance use disorder (i.e., within the last 6 months); significant risk for suicide; claustrophobia; daily nicotine use; self-reported use of antidepressants/other psychotropic medications; hormonal contraceptive use; peri- or postmenopausal signs; highly irregular periods; recent pregnancy or breastfeeding (i.e., within the last 6 months); illicit drug use within 4 weeks of participation. All eligible participants self-reported that they had not used antidepressants or other psychotropic medications within a time frame based on the half-life of that particular drug (e.g., had not used fluoxetine for at least 30 days prior to participation). Many of the participants had previously taken antidepressant medications and reported a variety of reasons (e.g., side effects) for not currently taking medication. Note, participants did not receive psychotherapeutic treatment as part of this study nor was psychotherapy an exclusionary criterion. To confirm no illicit drug use, we performed urine drug tests during three of the seven study visits (diagnostic interview and two fMRI scans). We tested for marijuana, cocaine, opiate, methamphetamine, and amphetamine. We also asked participants about illicit drug use during every study session.

All participants were recruited from the Madison, WI area via advertisements sent to counseling centers and clinics as well as paper and digital flyers posted in the community and online. Participants provided written informed consent in accordance with the University of Wisconsin Health Sciences Institutional Review Board IRB and were paid for their participation.

Table 1
Demographics by depression group.

	NoDep (n = 30)	PastDep (n = 15)	CurrentDep (n = 34)
Age	27.1 (7.6)	28.0 (5.8)	27.9 (7.1)
Education Level[a]			
High school diploma/ equivalent	0	1	0
Some college, no degree	12	4	10
Associate's degree	1	1	1
Bachelor's degree	7	6	11
Master's degree	8	3	10
Doctoral degree	2	0	2
Race[a]			
White	22	13	25
Asian	5	2	6
Black	3	0	1
Unknown	0	0	2
BDI-II – Placebo Day	0.9 (1.5)	1.3 (2.2)	20.3 (10.8)[b]

Notes. BDI-II = Beck Depression Inventory-II

[a] There were no significant differences between depression groups in education level ($\chi^2(10) = 7.48$, $p > .6$) or race ($\chi^2(4) = 3.32$, $p > .5$).

[b] BDI-II scores ranged from 0 to 47; as expected, we found significant differences between groups in depression severity ($F_{2,76} = 68.69$, $p < .001$).

2.2. Depression measure

To assess depression severity, participants completed the Beck Depression Inventory-II (BDI-II) at each visit [61]. The BDI-II is 21-item self-report inventory used to measure depression-related symptom severity during the past two weeks. The BDI-II score collected during the placebo day fMRI scan visit was used for all analyses.

2.3. fMRI data acquisition

All participants were scanned using a 3 T GE MRI scanner (Discovery MRI 750; GE Medical Systems, Waukesha, WI) equipped with an 8-channel radiofrequency coil array (GE Healthcare, Waukesha, WI). The resting-state fMRI data were collected using T2 * -weighted Echo Planar Imaging (EPI) sequence (TR/TE/FA: 2150 ms/22 ms/79°, matrix: 64 ×64, FOV: 22.4 cm, slice thickness: 3.5 mm, voxel size: 3.5 mm × 3.5 mm×3.5 mm, slices: 40 sagittal) using thin slices and short echo time in order to minimize signal dropout in the ventromedial prefrontal cortex. Each participant was instructed during the resting-state scan (~10 min) to remain "calm, still, and awake" with their eyes open fixating on a cross back-projected onto a screen via an LCD projector (Avotec, Stuart, FL). High-resolution T1-weighted structural imaging data were acquired using a weighted BRAVO pulse sequence (TI: 450 ms, TR/TE/flip angle (FA): 8.16 ms/3.2 ms/12°, matrix: 256 × 256 x 160, field of view (FOV): 215.6 mm, slice thickness: 1 mm, voxel size: 1 mm × 1 mm x 1 mm, slices: 156).

2.4. Preprocessing, motion analysis, and respiration for rs-fMRI data

The resting-state fMRI data were preprocessed using FSL tools (FMRIB software library; http://fsl.fmrib.ox.ac.uk/fsl/fslwiki/), AFNI [62] and ANTs (http://stnava.github.io/ANTs/). Initial preprocessing steps were performed using FSL MELODIC including removal of the first five volumes, interleaved slice-time correction, MCFLIRT motion correction, and spatial smoothing with a 6 mm full-width half-maximum (FWHM) Gaussian kernel.

ICA-FIX denoising was then applied to these data to extract and remove noise features from the data [e.g., motion, 63] as is common in BOLD signal variability preprocessing [e.g., 38]. Components were first hand-classified as either noise or signal from 8 randomly selected individuals from each depression group (n = 24) to create a training file of independent component noise features. We used previously published guidelines on hand-classification of components and examples of noise and signal components in ICA for fMRI data [63,64]. In addition, we provide some examples of hand-classified noise components from the present study in the Supplementary Materials (Figs. S4-S5). The training file of independent noise features was then used to regress out common noise components across all participants. Regression of the Friston 24 motion parameters and linear detrending were additionally applied during ICA-FIX denoising. Prior research has demonstrated that denoising using ICA-FIX can reduce non-neuronal BOLD signal

variability and enhance effect sizes for investigating between group differences in BOLD signal variability [27,65].

We also calculated average root mean squared (RMS) displacement as a summary measure of subject motion to include in all BOLD signal variability analyses as a covariate [as in 38]. Note, there were no significant differences in RMS motion between either the three-level ($F_{2,76} = 0.49$, $p = .61$) or two-level ($t(76) = 0.71$, $p = .48$) depression history groups. In addition, there was no correlation between RMS and depression symptom severity ($r = -0.14$, $p = .21$).

Subsequent preprocessing with the noise-cleaned data in ANTS and AFNI included realignment, co-registration to T1-weighted anatomical, normalization to MNI space using a symmetric normalization algorithm in ANTs [66], and despiking (3dDespike in AFNI). Cerebrospinal fluid (CSF), white matter (WM), and gray matter (GM) masks were segmented from normalized T1 anatomical images using FAST in FSL [67]. Lastly, CSF and WM masks were used in nuisance signal regression and data were bandpass filtered to reflect the low frequency neuronal fluctuations that distinguish resting-state BOLD activity (0.01 – 0.10 Hz).

Respiratory data were acquired using a pneumatic belt placed around the participant's chest just above the level of the diaphragm. This respiration belt is supplied by the scanner manufacturer (General Electric, Waukesha, WI), and the respiration measure is linearly related to the expansion of the belt. Respiration volume per time (RVT) were computed by first finding the peaks (maxima) and troughs (minima) of each breath. The distance between peaks was used as a measure of the respiration period. The series of maxima, minima, and periods were then interpolated to the imaging TR. RVT was computed as the (maxima – minima)/period at each TR [68]. Respiration data were missing for 1 participant. Importantly, there were no significant group differences in RVT, either for the three-level ($F_{2,75} = 2.77$, $p = .07$) or two-level depression history groups ($t(76) = -0.45$, $p = .66$). There was also no correlation between RVT and depression symptom severity ($r = -0.11$, $p = .33$).

2.5. Voxelwise BOLD signal variability

BOLD signal variability was calculated for all subjects as the voxelwise standard deviation (SD) of the BOLD signal across the entire time series (3dTstat in AFNI).

$$s = \sqrt{\frac{\sum_{i=1}^{n-1} (x_i - \bar{x}_i)^2}{n-1}}$$

2.6. Statistical analyses

2.6.1. Group differences in BOLD signal variability

To examine differences in BOLD signal variability between individuals with varying depression histories, we performed two separate group analyses. First, we conducted a one-way between-subjects analysis of covariance (ANCOVA) with three depression history groups (NoDep, PastDep, CurrentDep) predicting the voxelwise resting-state BOLD signal variability (3dMVM in AFNI). Second, we conducted a multivariate independent samples *t*-test with two depression history groups (NoDep, DepHist) predicting the voxelwise resting-state BOLD signal variability (3dttest++). As recommended by previous BOLD signal variability research, RMS motion was included as a covariate in each group analysis [33,37,38]. All analyses were family-wise error (FWE) cluster-corrected at the whole-brain level [69,70], with a predefined voxelwise threshold of $p < .001$ (uncorrected) with a cluster-corrected voxel size of ≥ 38 voxels significant at $p_{FWE} < 0.05$. Results were overlaid on the normalized mean anatomical image. Effect sizes and 95% confidence intervals (CI) were reported for all significant results. We also conducted an a priori power analysis based on our independent samples *t*-test results (NoDep vs. DepHist) using G*Power version 3.1 [71]. Based on this a priori power analysis, a sample size of between about 38–54 would be needed to achieve a power of.95 with an effect size of between 1.27 and 1.05, as reported below in the results. In addition, we evaluated the data for extreme outliers (>3 interquartile range) in RStudio 1.2.5033.

2.6.2. Relationship between BOLD signal variability and depression severity

To investigate the relationship between depressive symptom severity measured continuously and resting-state BOLD signal variability across the sample, we conducted a multivariate multiple linear regression analysis (3dttest++ in AFNI). The model assessed the relationship between resting-state voxelwise SD of the BOLD signal and depression severity as indicated by BDI-II scores. RMS motion was also included as a covariate in the regression model. As in the ANCOVA described above, all analyses were FWE cluster-corrected at the whole-brain level ($p_{FWE} < 0.05$). Results were overlaid on the normalized mean anatomical image.

2.6.3. Machine learning classification modeling using random forest

We utilized a random forest (RF) classification algorithm to determine whether BOLD signal variability features could be used to predict depression group membership in two separate algorithms (1: NoDep, PastDep, CurrentDep; 2: NoDep, DepHist). RF modeling was selected for its accuracy, unbiased estimates, ability to balance error in unbalanced datasets, and ability to estimate variable importance [72,73]. All modeling was performed in RStudio 1.2.5033.

We selected 24 ROIs from the DMN, SN, and FPN based on previous research [see Table 2; 74,75], as these networks have been consistently shown to be altered in depression [8,9,11,14]. The coordinates for these ROIs were used to create 6-mm radius seed masks in MNI space. The transformation matrix from the registration procedure was used to align each seed ROI mask to each participant's fully preprocessed fMRI data in MNI space. Next, we calculated the average SD of BOLD signal across all voxels within the ROI mask (3dROIstats). Thus, 24 features were collected for the algorithm, i.e., BOLD resting-state BOLD signal variability for the 24 seeds from the DMN, SN, and FPN. Seventy percent of these data were then randomly selected and bootstrapped for a training dataset to create and tune the model, and the remaining 30% of the data were placed in a testing dataset for later model evaluation (Supplementary Fig. S1).

To evaluate each model's performance, we applied the RF classifier to the testing dataset and created a confusion matrix to calculate sensitivity, specificity, and accuracy for each level of depression history. From this matrix, we also calculated the overall accuracy for the model's predictions and created receiver operator characteristic (ROC) curves. We used two measures to evaluate variable importance for the BOLD signal variability of different network seeds: mean decrease in accuracy (MDA) and mean decrease in impurity, also known as Gini importance (Gini). Both of these measures look at the unique influence of randomly permuting the values of a single feature on the overall accuracy of predictions. Features with larger positive values for both measures then indicate a variable with greater discriminative power and predictive value.

As is common in machine learning, model optimization was also included to achieve higher rates of classification accuracy. A default model was first established with all standard parameters, including the number of features tried for each decision point of the forest (6) and for the total number of trees in the forest (500). After evaluating the default model's performance, we applied common tuning methods to increase the model's accuracy: increase the total number of trees, increase the number of features at each node, apply a random search to the number of features at each node, apply cross-validation folding techniques to training data [72,76,77].

Table 2
Resting-state networks ROI coordinates.

DMN ROI	x	y	z	SN ROI	x	y	z	FPN ROI	x	y	z
Pc	-5	-62	48	In R	42	10	-12	dlPFC R	46	46	14
PCC	-5	-54	21	In L	-40	18	-12	dlPFC L	-34	46	6
vACC	3	36	-9	dACC R	6	22	30	IPS R	38	-56	44
IPL R	53	-29	23	dACC L	-6	18	30	IPS L	-48	-48	48
IPL L	-58	-38	28	FP L	-24	56	10	ITG R	58	-54	-16
mPFC	-2	53	21	vlPFC R	42	46	0	vlPFC R	34	56	-6
MTG R	45	-68	14	dlPFC R	30	48	22	vlPFC L	-32	54	-4
MTG L	-42	-68	16	dlPFC L	-38	52	10	dmPFC	0	36	46

Notes. MNI coordinates of resting-state network regions of interest. dACC, dorsal anterior cingulate cortex; dlPFC, dorsolateral prefrontal cortex; DMN, default mode network; dmPFC, dorsomedial prefrontal cortex; FP, frontal pole; FPN, frontoparietal network; In, insula; IPL, inferior parietal lobule; IPS, intraparietal sulcus; ITG, inferior temporal gyrus; MFG, middle frontal gyrus; mPFC, medial prefrontal cortex; MTG, middle temporal gyrus; Pc, precuneus; PCC, posterior cingulate cortex; ROI, region of interest; SN, salience network; vACC, ventral anterior cingulate cortex; vlPFC, ventrolateral prefrontal cortex.

3. Results

3.1. Differences in BOLD signal variability based on depression history

Based on the analysis comparing three levels of depression history, we found group differences in BOLD signal variability in the right and left cerebellum ($p < .001$, uncorrected; Table 3). Post hoc comparisons indicated that these findings were driven by the current depression group. Individuals with no history of depression had greater BOLD signal variability than those with current depression in the right and left cerebellum (Table 3). However, these results did not survive FWE cluster-correction.

In the second group analysis, we compared individuals with no history of depression to those with any history of depression. We identified significant differences in BOLD signal variability in the left cerebellum ($t(43.41) = 4.59$, $p < .001$, $d = 1.18$, CI = 1.24–3.17), right cerebellum ($t(39.77) = 4.78$, $p < .001$, $d = 1.27$, CI = 1.42–3.51), and right inferior parietal lobule (IPL) extending to superior parietal lobule ($t(38.90) = 3.95$, $p < .001$, $d = 1.05$, CI = 2.15–6.68). Specifically, there was decreased neural signal variability across all clusters for those with a history of depression (either past or current; Fig. 1b). These results survived FWE correction ($p_{FWE} < 0.05$; Table 3; Fig. 1a), were corrected for unequal variances between groups based on Levene's test ($ps = 0.01$–0.001), and remained significant after removing two outliers (all $ps < 0.001$).

Table 3
Group differences in BOLD signal variability based on depression history.

Cluster location	MNI coordinates (x, y, z)	Cluster size	Test value
Full ANCOVA model with 3 depression groups[a]			*F* value
R. cerebellum vermal lobule VIII	17, − 63, − 51	9	14.94 *
L. cerebellum vermal lobule VIII	-19, − 69, − 51	7	11.79 *
Posthoc comparison: no history of depression vs. current depression[a]			*t* value
R. cerebellum vermal lobule VIII	17, − 63, − 40	15	5.29 *
L. cerebellum vermal lobule VIII	-19, − 69, − 54	10	4.69 *
Independent samples *t*-test with 2 depression groups[b]			*t* value
L. cerebellum vermal lobule VI extending to lobule VII	-7, − 69, − 24	89	5.07 * *
R. cerebellum vermal lobule VIII	12, − 60, − 51	48	5.44 * *
R. inferior parietal lobule extending to superior parietal lobule	32, − 45, 54	40	4.53 * *

Notes.
*Results at uncorrected threshold, $p < .001$.
* *Results significant after family-wise error cluster correction, $p_{FWE} < 0.05$.
[a] Full ANCOVA model with 3 depression groups included no history of depression, past history of depression, and current depression groups. Posthoc comparison of no history of depression versus current depression groups showed similar results to the full model.
[b] Multivariate independent samples *t*-test with 2 depression groups compared no history of depression and past history of depression groups.

3.2. Relationship between BOLD signal variability and depression severity

Depression severity was negatively related to BOLD signal variability in the right and left cerebellum ($p < .001$, uncorrected; Fig. 2). In other words, greater depression severity was associated with lower BOLD signal variability within the two cerebellar clusters. However, these results did not survive FWE cluster correction.

3.3. Machine learning classification of depression with BOLD signal variability

The distribution of BOLD signal variability features within the three levels of depression history for the DMN, SN, and FPN seeds are shown in Fig. 3a. Using the three depression history levels, the random forest algorithm achieved an overall accuracy of 63.63% and within class sensitivity and specificity ranging from 60.61% to 85.41% (Table 4; Supplementary Fig. S2). The top 15 most important BOLD signal variability features to model classification revealed regions within the DMN, SN, and FPN (Fig. 3b-c). The two most important features were the vACC and left middle temporal gyrus (MTG) of the DMN (Fig. 3c).

For the second algorithm, we used the classifications of no history of depression and any history of depression. The distribution of BOLD signal variability features within these two depression history groups are shown in Fig. 4a. This model achieved 73.96% accuracy distinguishing between the two classes, with 77.58% sensitivity and 72.96% specificity (Table 5; Supplementary Fig. S3). The top 15 most important BOLD signal variability features included regions within the DMN, SN, and FPN (Fig. 4b-c). Similar to the algorithm with three depression history groups, the vACC and left MTG of the DMN were the two regions with the most predictive power in the model (Fig. 3c).

4. Discussion

To our knowledge, this is the first study to investigate the predictive value of resting-state BOLD signal variability in unipolar depressive disorders. The present study examined depression history and severity in relation to BOLD signal variability as reflected by the standard deviation of resting-state voxelwise BOLD signal. Additionally, we evaluated the importance of resting-state BOLD signal variability measures in predicting depression history using random forest ML classification algorithms.

Partially in line with the first hypothesis, we determined that individuals with a history of depression had significantly lower resting-state BOLD signal variability compared to individuals with no history of depression. This difference was localized to three regions: the right and left cerebellar vermis and a region extending from the right IPL to the right superior parietal lobule. Furthermore, greater depression

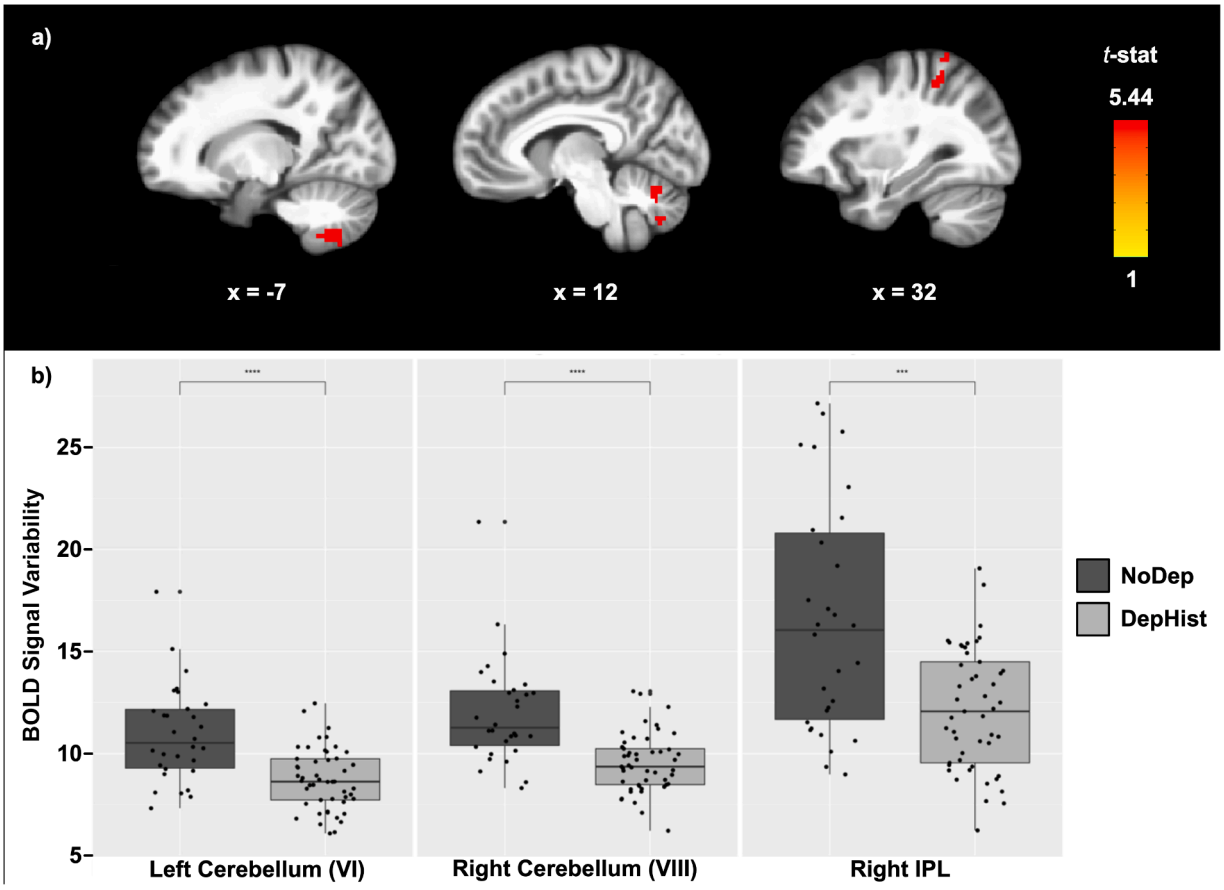

Fig. 1. Depression history was associated with BOLD signal variability in bilateral cerebellum and right IPL. a) Results from multivariate two sample *t*-test shows greater resting-state voxelwise BOLD signal variability in individuals with no history of depression compared with individuals with any history of depression (p_{FWE} <0.05). Color bar depicts *t*-values. b) Bar graphs with individual data points plot average BOLD signal variability in left cerebellum, right cerebellum, and right IPL for individuals with no history of depression (dark gray) and a past history of depression (light gray). Abbreviations: IPL = inferior parietal lobule.

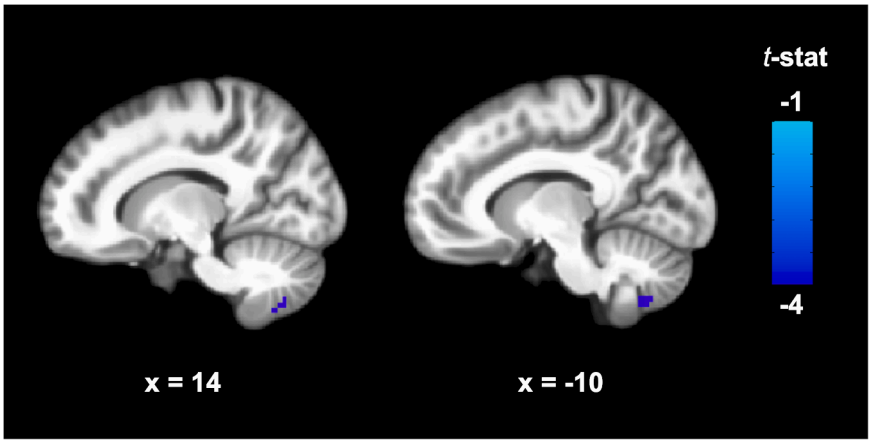

Fig. 2. Depression severity and reduced BOLD signal variability. Results from multivariate multiple linear regression reveals negative correlation between resting-state voxel-wise BOLD signal variability and depressive symptom severity ($p < .001$, uncorrected). These results did not survive multiple comparisons correction (p_{FWE} <0.05). Color bar depicts *t*-values.

severity was associated with lower BOLD signal variability within the two cerebellar regions. Although this latter finding did not survive cluster correction, the locations of the two cerebellar regions were consistent with the initial analyses and reflected the expected direction of the second hypothesis. Thus, the main finding for these two analyses was that individuals with depression exhibited lower resting-state BOLD signal variability in the cerebellum and right lateral parietal cortex.

These areas of lower BOLD signal variability for those with depression are consistent with previous literature investigating alterations in activity and connectivity in depression. For instance, the two clusters found in the left and right vermis of the cerebellum mirror early findings on "cerebellar cognitive affective syndrome" [78]. This syndrome, typically found in individuals with cerebellar damage, is associated with cognitive and affective symptoms overlapping with depression, such as

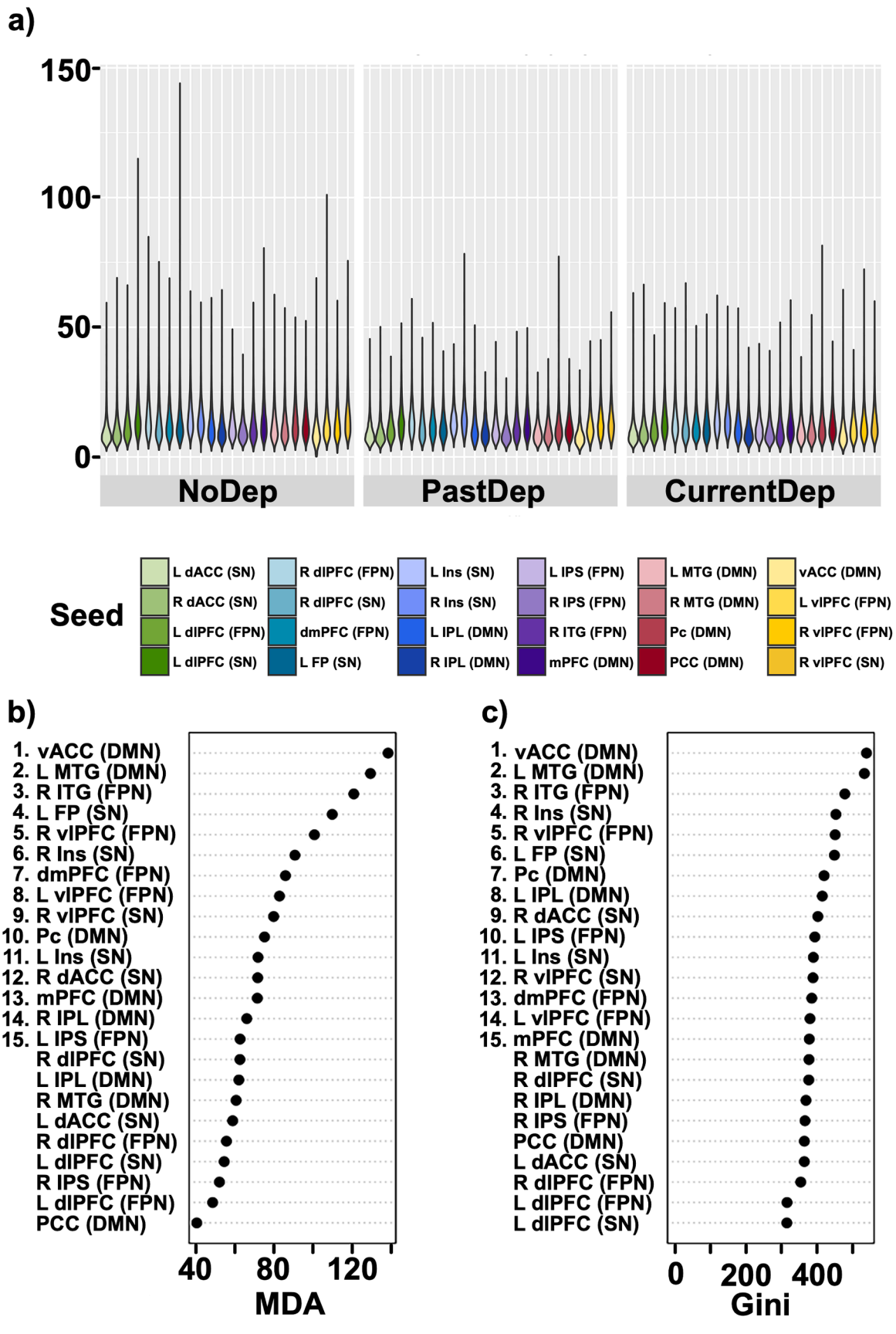

(caption on next page)

Fig. 3. Random forest classification predicts three-level depression groups for BOLD signal variability in DMN, SN, and FPN. a) Violin plots illustrating the distribution of BOLD signal variability features for DMN, SN, and FPN seeds for the three levels of depression history visually show differences in variability in no history and past and current depression history groups. b) Variable importance plot of MDA for the three-level depression history classification random forest algorithm showing equal representation of DMN, SN, and FPN seeds. c) Variable importance plot of Gini importance for the three-level depression history classification random forest algorithm. The top 15 most important BOLD signal variability features for the three-level classification of depression included regions within the DMN, SN, and FPN (b-c). Abbreviations: dACC, dorsal anterior cingulate cortex; dlPFC, dorsolateral prefrontal cortex; DMN, default mode network; dmPFC, dorsomedial prefrontal cortex; FP, frontal pole; FPN, frontoparietal network; In, insula; IPL, inferior parietal lobule; IPS, intraparietal sulcus; ITG, inferior temporal gyrus; MFG, middle frontal gyrus; mPFC, medial prefrontal cortex; MTG, middle temporal gyrus; Pc, precuneus; PCC, posterior cingulate cortex; ROI, region of interest; SN, salience network; vACC, ventral anterior cingulate cortex; vlPFC, ventrolateral prefrontal cortex.

Table 4
Confusion matrix and evaluation metrics for the 3-level depression history random forest model.

Confusion Matrix	*Reference*			Within Class Evaluation Metrics	
Prediction	NoDep	PastDep	CurrDep	*Sensitivity*	*Specificity*
NoDep	1562	62	851	66.69	78.13
PastDep	282	360	595	71.43	85.41
CurrDep	498	82	2225	60.61	79.62

Notes. Confusion matrix and within class evaluation metrics for random forest model using 3 levels of depression history. NoDep = no history of depression; PastDep = previous history of depression; CurrDep = current depression.

executive dysfunction and flat affect. In addition, studies of patients diagnosed with affective disorders reveal significantly higher rates of vermal atrophy in comparison to healthy controls [79]. In individuals with depression, structural and functional abnormalities in the vermis have been frequently reported [80]. Together these studies implicate the posterior lobe of the cerebellum in the pathophysiology of depression.

In terms of specific cerebellar anatomy, the current findings of lower BOLD signal variability were localized to lobules VI, VII, and VIII for those with a history of depression. Lobule VII has often shown functional connections with regions of the DMN, while lobules VI and VIII have more often been associated with emotion processing regions [80]. Previous work has demonstrated that individuals with depression have significantly decreased rsFC between lobule VII and regions of the DMN, FPN, and reward circuit in comparison to controls [80–82]. Likewise, a study using seed-based rsFC with various cerebellar ROIs found significantly reduced connectivity between lobules VI and VIII and the IPL, prefrontal cortex, and inferior temporal gyrus [83]. The cerebellar dysfunction found in these studies using average BOLD signal measures was later replicated in analyses using neural signal variability measures (e.g., amplitude low frequency fluctuations, ALFF; fractional ALFF, fALFF). For example, Song and colleagues [84] found significantly lower ALFF and fALFF values in the left cerebellum of a patient group with major depressive disorder compared to a healthy control group. In another study, lower ALFF in the right cerebellum was identified in individuals with first-episode major depressive disorder [85]. Comparable changes in fALFF values were also found in the right vermis for individuals with treatment-resistant depression [86]. A recent meta-analysis of resting-state fMRI ALFF studies further revealed decreased ALFF in bilateral cerebellum in major depressive disorder [87]. This evidence of disrupted cerebellar activity is consistent with our findings, suggesting that the activity and function of the vermis may be associated with depression.

BOLD signal variability differences were not limited to the cerebellum, however. The direct comparison of those with no history of depression to those with a history of depression revealed a third region of BOLD signal variability differences in the right lateral parietal cortex. Within this region extending from the right IPL to the superior parietal lobule, participants with a history of depression exhibited significantly less BOLD signal variability. In terms of the function of these regions, previous research has consistently associated the IPL with DMN function, with roles in emotion perception and sensory integration [88–92]. The IPL was also recently implicated in the inhibition of mind wandering in healthy subjects through its connections with the PCC [93]. With regard to individuals with depression, the IPL has consistently shown increased activity as well as increased connectivity with other DMN regions involved in self-related thought [10–13,17]. In contrast, the superior parietal lobule is associated with attention to external stimuli, with connections to both FPN and SMN regions, and is involved in visuospatial perception and reasoning, working memory, and attention [10–13,94]. The superior parietal lobule has shown lower inverse correlations with DMN regions in individuals with depression in comparison to controls [9,14,18]. Studies using neural signal variability measures have also found functional differences in the right IPL and superior parietal lobule in depression. For example, Wang et al. [95] found that patients with major depressive disorder had significantly lower fALFF values in the right IPL compared to controls. These results were congruent with a later study that reported significantly lower ALFF and fALFF values in bilateral superior parietal lobule and right IPL for those with depression compared to healthy individuals [84,86,96]. This previous work in conjunction with the current results indicates that individuals with a history of depression have aberrant neural activity, connectivity, and BOLD signal variability within the posterior cerebellum and right lateral parietal cortex.

An important question for future research will be to determine how BOLD signal variability relates to network connectivity in depression. Research in healthy populations suggests that lower local temporal variability is associated with reduced network integration [24]. Other studies have shown that the relationship between BOLD signal variability measures and functional connectivity strength can vary within and between networks [97,98]. Thus, it is possible that lower BOLD signal variability of DMN regions in the present study may contribute to hyperconnectivity of DMN reported in individuals with depression [11,13,17]. Consistent with this hypothesis, Fu and colleagues [98] found that lower local BOLD signal variability was associated with greater dynamic functional connectivity strength within the DMN. However, additional research will be required to investigate the relationships between within-network signal variability and resting-state functional connectivity in depression.

Considering these neurobiological differences in depression history, in the final analysis we evaluated the predictive value of BOLD signal variability measures in classifying individuals by depression history. In line with our third hypothesis, the BOLD signal variability features of the DMN, SN, and FPN provided predictive value in both random forest ML models. Across both depression group models, the two most important regions for classification within the DMN were the vACC and left MTG. As for the SN, the frontal pole and insula were consistently important. Lastly, the ventrolateral prefrontal cortex and ITG were most important in the FPN.

Although the random forest model did not explicitly indicate whether there was greater or reduced BOLD signal variability in these network regions for individuals with a history of depression, the locations of these brain regions parallel previous fMRI studies using ALFF and fALFF measures. For instance, the vACC of the DMN has been implicated in the pathophysiology of depression [5–7,10] and consistently associated with increased ALFF in patients with major depressive disorder versus healthy comparison participants [87]. In addition, depressed individuals frequently exhibit decreased fALFF and ALFF of the MTG within the DMN [95,99]. With regard to the important regions

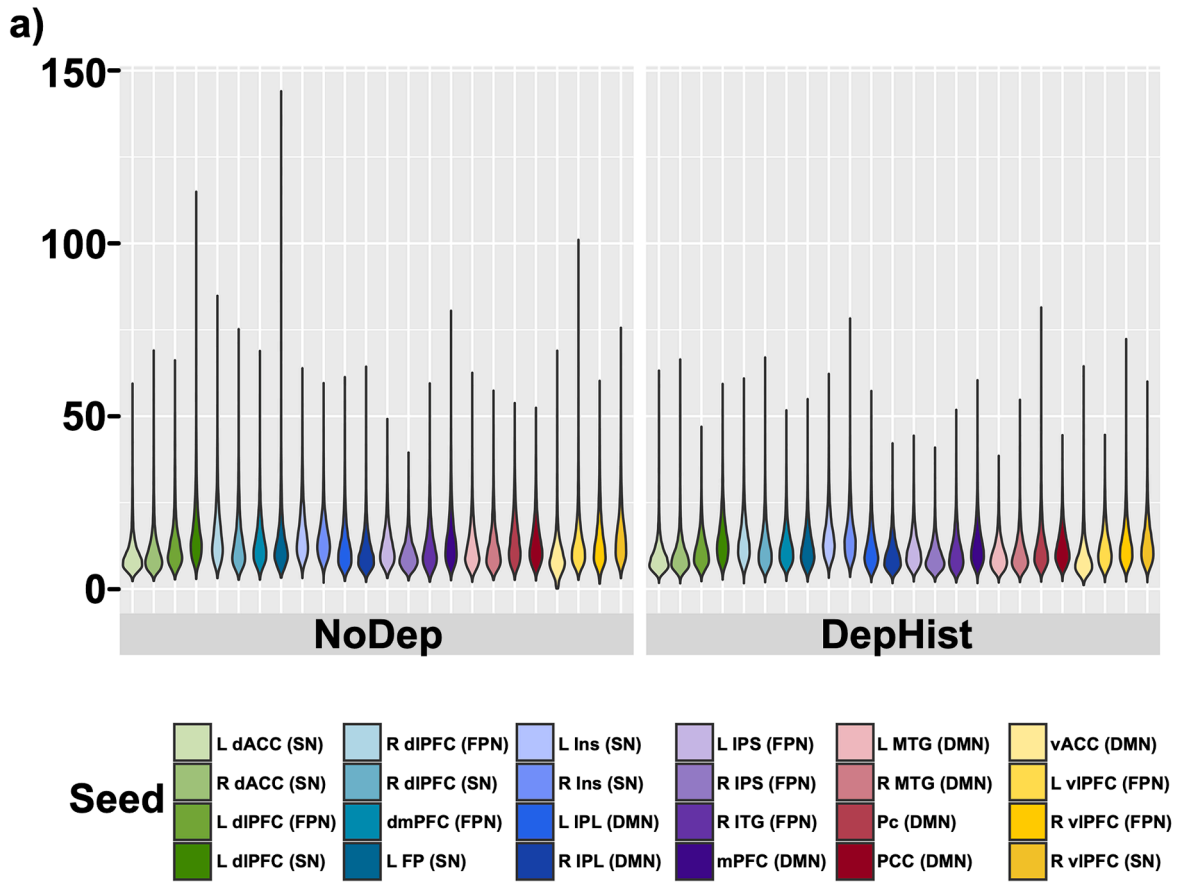

(caption on next page)

Fig. 4. Random forest classification predicts two-level depression groups with BOLD signal variability in DMN, SN, and FPN. a) Violin plots illustrating the distribution of BOLD signal variability features for DMN, SN, and FPN seeds for the two levels of depression history visually show differences in variability in no history and any depression history groups. b) Variable importance plot of MDA for the two-level depression history classification random forest algorithm showing equal representation of DMN, SN, and FPN seeds. c) Variable importance plot of Gini importance for the two-level depression history classification random forest algorithm. Similar to the three-level depression history algorithm, the top 15 most important BOLD signal variability features for the two-level classification of depression included regions within the DMN, SN, and FPN (b-c). Abbreviations: dACC, dorsal anterior cingulate cortex; dlPFC, dorsolateral prefrontal cortex; DMN, default mode network; dmPFC, dorsomedial prefrontal cortex; FP, frontal pole; FPN, frontoparietal network; In, insula; IPL, inferior parietal lobule; IPS, intraparietal sulcus; ITG, inferior temporal gyrus; MFG, middle frontal gyrus; mPFC, medial prefrontal cortex; MTG, middle temporal gyrus; Pc, precuneus; PCC, posterior cingulate cortex; ROI, region of interest; SN, salience network; vACC, ventral anterior cingulate cortex; vlPFC, ventrolateral prefrontal cortex.

Table 5
Confusion matrix for the 2-level depression history random forest model.

Confusion Matrix	*Reference*	
Prediction	NoDep	DepHist
NoDep	1094	1381
DepHist	316	3726

Notes. Confusion matrix for random forest model using 2 levels of depression history. NoDep = no history of depression; DepHist = any history of depression (past or current).

of the SN, reduced ALFF values within the insula have been reported for increased Hamilton Depression Rating Scale scores in adolescents and young adults with major depressive disorder [100]. As for the FPN, individuals with depressive symptoms have presented decreased ALFF in the ventrolateral prefrontal cortex but increased fALFF in the ITG [95,101]. Given these findings, it is possible that the regions that were most important for classifying depression history in the random forest models have increased BOLD variability for vACC but decreased BOLD signal variability in other network regions for those with a history of depression. With the exception of the vACC, the pattern of reduced neural signal variability in depression mirrors both the violin plot visualizations of the BOLD signal variability features (Figs. 3a and 4a) as well as our earlier findings of lower BOLD signal variability in the cerebellum and right parietal cortex for individuals with a history of depression.

To summarize, individuals with a history of depression demonstrated lower BOLD signal variability in cerebellar and lateral parietal regions. In addition, ML demonstrated that BOLD signal variability has moderate predictive value in categorizing depressed versus healthy groups and identified vACC and left MTG of the DMN as the most important regions in differentiating depressed from healthy individuals. Importantly, these results are consistent with several previous large-scale structural and functional neuroimaging studies reporting depression-related changes in DMN [102–106]. Further, these findings extend prior research demonstrating that measures of BOLD signal variability are an important source of information with regard to disordered affect. Furthermore, the regions identified with standard [parametric] statistics and with ML suggest that neural signal variability in brain areas involved in emotion processing, self-reference, and working memory, should be investigated in future research on depression.

Some limitations are worth noting for this study. First, a few concerns arise from the size of the sample ($N = 79$). Several recent reviews have discussed the importance of large sample sizes for ML classification [107–110]. In general, the use of smaller sample sizes may decrease the accuracy and generalizability of ML algorithms. In addition, the smaller sample size and use of only one resting-state scan could limit the reliability and reproducibility of our findings [111,112]. However, previous studies examining different resting-state and task-based fMRI metrics have reported moderate to high test-retest reliability for BOLD signal variability/ALFF [36,113,114]. Nevertheless, subsequent research using larger sample sizes and assessing test-retest reliability will be necessary to replicate these results. Second, the sample sizes for the depression history groups were unequal and the assumption of homogeneity of variance was not met for BOLD signal variability in the cerebellum and IPL clusters. Although these findings remained significant after correcting for unequal variances between groups, additional research with equal numbers of participants in each depression history group could be used to corroborate these findings. Third, this sample included only female participants. Thus, it is unclear if the differences in BOLD signal variability observed in this study would replicate for males with depression. Future studies could investigate whole-brain, gender-based differences in BOLD signal variability as well as gender-based differences specific to depressive disorders. Fourth, we focused on resting-state BOLD signal variability in the current study. However, research suggests that task-based BOLD signal variability may outperform resting-state BOLD signal variability measures. For example, a recent study comparing resting-state and task-based BOLD signal variability showed that task-based signal variability was the strongest predictor of treatment outcomes for individuals with social anxiety disorder [115]. Therefore, additional research will be necessary to compare task-based and resting-state BOLD signal variability in depression. Fifth, the present study did not consider the interaction between age and depression in relation to BOLD signal variability. Although there were no significant differences between depression history groups in terms of age ($F(2, 76) = 0.14$, $p > .05$), previous studies using BOLD signal variability have found age-related functional differences across the lifespan [27,31–33]. Therefore, it may be important to examine the interaction between age and depression in relation to BOLD signal variability in future research.

Considering the high prevalence of depressive disorders [2,3], the current findings may have important clinical implications for interventions designed to restore optimal neural function in depression. In particular, repetitive transcranial magnetic stimulation (rTMS) applied to the right parietal cortex and cerebellum appears promising for alleviating depressive symptoms. Compared to individuals given a sham rTMS treatment, individuals given 10 sessions of 2 Hz rTMS to the right parietal cortex presented higher rates of clinical response with 50% or higher reductions in Hamilton Rating Scale for Depression (HAMD) scores [116]. Repetitive TMS applied to the medial cerebellum similarly resulted in reduced depressive mood and increased attention in healthy individuals [117–119]. Aside from treatment implications, our findings also highlight a neurobiological correlate of depression that may underlie other psychiatric conditions that have high comorbidity with depressive disorders, such as posttraumatic stress disorder [120]. From this perspective, future research could adopt a transdiagnostic approach and assess the role of neural signal variability in the severity of various psychiatric symptoms.

5. Conclusion

In conclusion, the current study demonstrates that differences in BOLD signal variability exist between individuals with a history of depression and individuals with no history of depression. The lower resting-state BOLD signal variability found in the cerebellum and right lateral parietal cortex for those with depression highlights a potential indicator of decreased resting-state network integration and neural dysfunction in depressive disorders. More broadly, these findings provide support for this novel approach to investigating aberrant neural activity in depression and provide a better understanding of the resting-state neural correlates of depression.

CRediT authorship contribution statement

Sally Pessin: Conceptualization, Methodology, Formal analysis, Writing – original draft, Visualization, Writing – reviewing & editing. **Erin C. Walsh**: Project administration, Methodology, Investigation, Data curation, Writing – review & editing. **Roxanne M. Hoks**: Project administration, Methodology, Investigation, Data curation, Writing – review & editing. **Rasmus M. Birn**: Methodology, Investigation, Data curation, writing – review & editing. **Heather C. Abercrombie**: Funding acquisition, Methodology, Investigation, Data curation, Writing – review & editing. **Carissa L. Philippi**: Conceptualization, Methodology, Data curation, Software, Formal analysis, Writing – reviewing & editing, Supervision.

Conflicts of interest

The authors report no biomedical financial interests or potential conflicts of interest.

Data Availability

The data that support the findings of this study are available from the corresponding author upon reasonable request

Acknowledgements

We thank the participants for their time and effort in making this research possible. This study was funded by grants awarded to HCA by the National Institute of Mental Health (R01MH094478), the University of Wisconsin-Madison Office of the Vice Chancellor for Research and Graduate Education with funding from the Wisconsin Alumni Research Foundation, and the University of Wisconsin-Madison Women in Science and Engineering Leadership Institute/The Office of the Provost. EW was supported by the National Center for Advancing Translational Sciences, National Institutes of Health (KL2TR001109). The content is solely the responsibility of the authors and does not necessarily represent the official views of the National Institutes of Health.

Appendix A. Supporting information

Supplementary data associated with this article can be found in the online version at doi:10.1016/j.bbr.2022.113999.

References

[1] American Psychiatric Association, Diagnostic and Statistical Manual of Mental Disorders: DSM-5, American Psychiatric Association, Washington, D.C., 2013.
[2] A.J. Ferrari, F.J. Charlson, R.E. Norman, S.B. Patten, G. Freedman, C.J.L. Murray, T. Vos, H.A. Whiteford, Burden of depressive disorders by country, sex, age, and year: findings from the global burden of disease study 2010, PLoS Med. 10 (2013), e1001547, https://doi.org/10.1371/journal.pmed.1001547.
[3] World Health Organization, Depression and other common mental disorders: global health estimates, World Health Organization, Geneva, 2017.
[4] S.L. Burcusa, W.G. Iacono, Risk for recurrence in depression, Clin. Psychol. Rev. 27 (2007) 959–985, https://doi.org/10.1016/j.cpr.2007.02.005.
[5] W.C. Drevets, J.L. Price, M.L. Furey, Brain structural and functional abnormalities in mood disorders: implications for neurocircuitry models of depression, Brain Struct. Funct. 213 (2008) 93–118, https://doi.org/10.1007/s00429-008-0189-x.
[6] H.S. Mayberg, Limbic-cortical dysregulation: a proposed model of depression, J. Neuropsychiatry Clin. Neurosci. 9 (1997) 471–481, https://doi.org/10.1176/jnp.9.3.471.
[7] H.S. Mayberg, Positron emission tomography imaging in depression: a neural systems perspective, Neuroimaging Clin. 13 (2003) 805–815, https://doi.org/10.1016/S1052-5149(03)00104-7.
[8] V. Menon, Large-scale brain networks and psychopathology: a unifying triple network model, Trends Cogn. Sci. 15 (2011) 483–506, https://doi.org/10.1016/j.tics.2011.08.003.
[9] D.A. Pizzagalli, Frontocingulate dysfunction in depression: toward biomarkers of treatment response, Neuropsychopharmacology 36 (2011) 183–206, https://doi.org/10.1038/npp.2010.166.
[10] M. Greicius, B.H. Flores, V. Menon, G.H. Glover, H.B. Solvason, H. Kenna, A. L. Reiss, A.F. Schatzberg, Resting-state functional connectivity in major depression: abnormally increased contributions from subgenual cingulate cortex and thalamus, Biol. Psychiatry 62 (2007) 429–437, https://doi.org/10.1016/j.biopsych.2006.09.020.
[11] S. Whitfield-Gabrieli, J.M. Ford, Default mode network activity and connectivity in psychopathology, Annu. Rev. Clin. Psychol. 8 (2012) 49–76, https://doi.org/10.1146/annurev-clinpsy-032511-143049.
[12] L.M. Williams, Defining biotypes for depression and anxiety based on large-scale circuit dysfunction: a theoretical review of the evidence and future directions for clinical translation, Depress Anxiety 34 (2017) 9–24, https://doi.org/10.1002/da.22556.
[13] M.G. Berman, S. Peltier, D.E. Nee, E. Kross, P.J. Deldin, J. Jonides, Depression, rumination and the default network, Soc. Cogn. Affect. Neurosci. 6 (2011) 548–555, https://doi.org/10.1093/scan/nsq080.
[14] R. Kaiser, J. Andrews-Hanna, T. Wager, D. Pizzagalli, Large-scale network dysfunction in major depressive disorder: a meta-analysis of resting-state functional connectivity, JAMA Psychiatry 72 (2015) 603–611, https://doi.org/10.1001/jamapsychiatry.2015.0071.
[15] C.L. Philippi, M.D. Cornejo, C.P. Frost, E.C. Walsh, R.M. Hoks, R. Birn, H. C. Abercrombie, Neural and behavioral correlates of negative self-focused thought associated with depression, Hum. Brain Mapp. 39 (2018) 2246–2257, https://doi.org/10.1002/hbm.24003.
[16] Y.I. Sheline, D.M. Barch, J.L. Price, M.M. Rundle, S.N. Vaishnavi, A.Z. Snyder, M. A. Mintun, S. Wang, R.S. Coalson, M.E. Raichle, The default mode network and self-referential processes in depression, Proc. Natl. Acad. Sci. 106 (2009) 1942–1947, https://doi.org/10.1073/pnas.0812686106.
[17] X. Zhu, X. Wang, J. Xiao, J. Liao, M. Zhong, W. Wang, S. Yao, Evidence of a dissociation pattern in resting-state default mode network connectivity in first-episode, treatment-naive major depression patients, Biol. Psychiatry 71 (2012) 611–617, https://doi.org/10.1016/j.biopsych.2011.10.035.
[18] P.C. Mulders, P.F. van Eijndhoven, A.H. Schene, C.F. Beckmann, I. Tendolkar, Resting-state functional connectivity in major depressive disorder: a review, Neurosci. Biobehav. Rev. 56 (2015) 330–344, https://doi.org/10.1016/j.neubiorev.2015.07.014.
[19] A. Manoliu, C. Meng, F. Brandl, A. Doll, M. Tahmasian, M. Scherr, D. Schwerthöffer, C. Zimmer, H. Förstl, J. Bäuml, V. Riedl, A. Wohlschläger, C. Sorg, Insular dysfunction within the salience network is associated with severity of symptoms and aberrant inter-network connectivity in major depressive disorder, Front. Hum. Neurosci. 7 (2014) 930, https://doi.org/10.3389/fnhum.2013.00930.
[20] R. Ramasubbu, N. Konduru, F. Cortese, S. Bray, I. Gaxiola, B. Goodyear, Reduced intrinsic connectivity of amygdala in adults with major depressive disorder, Front. Psychiatry 5 (2014) 17, https://doi.org/10.3389/fpsyt.2014.00017.
[21] G.S. Alexopoulos, M.J. Hoptman, D. Kanellopoulos, C.F. Murphy, K.O. Lim, F. M. Gunning, Functional connectivity in the cognitive control network and the default mode network in late-life depression, J. Affect. Disord. 139 (2012) 56–65, https://doi.org/10.1016/j.jad.2011.12.002.
[22] C. Liston, A.C. Chen, B.D. Zebley, A.T. Drysdale, R. Gordon, B. Leuchter, H. U. Voss, B.J. Casey, A. Etkin, M.J. Dubin, Default mode network mechanisms of transcranial magnetic stimulation in depression, Biol. Psychiatry 76 (2014) 517–526, https://doi.org/10.1016/j.biopsych.2014.01.023.
[23] M. Tahmasian, D. Knight, A. Manoliu, D. Schwerthöffer, M. Scherr, C. Meng, J. Shao, H. Peters, A. Doll, H. Khazaie, A. Drzezga, J. Bäuml, C. Zimmer, H. Förstl, A. Wohlschläger, Riedl valentin, C. Sorg, Aberrant intrinsic connectivity of hippocampus and amygdala overlap in the fronto-insular and dorsomedial-prefrontal cortex in major depressive disorder, Front. Hum. Neurosci. 7 (2013) 639, https://doi.org/10.3389/fnhum.2013.00639.
[24] D.D. Garrett, S.M. Epp, A. Perry, U. Lindenberger, Local temporal variability reflects functional integration in the human brain, NeuroImage 183 (2018) 776–787, https://doi.org/10.1016/j.neuroimage.2018.08.019.
[25] L. Waschke, N.A. Kloosterman, J. Obleser, D.D. Garrett, Behavior needs neural variability, Neuron 109 (2021) 751–766, https://doi.org/10.1016/j.neuron.2021.01.023.
[26] A.Z. Burzynska, C.N. Wong, M.W. Voss, G.E. Cooke, E. McAuley, A.F. Kramer, White matter integrity supports BOLD signal variability and cognitive performance in the aging human brain, PLoS One 10 (2015), e0120315, https://doi.org/10.1371/journal.pone.0120315.
[27] D.D. Garrett, N. Kovacevic, A.R. McIntosh, C.L. Grady, Blood oxygen level-dependent signal variability is more than just noise, J. Neurosci. 30 (2010) 4914, https://doi.org/10.1523/JNEUROSCI.5166-09.2010.
[28] A.K. Easson, A.R. McIntosh, BOLD signal variability and complexity in children and adolescents with and without autism spectrum disorder, Dev. Cogn. Neurosci. 36 (2019), 100630, https://doi.org/10.1016/j.dcn.2019.100630.
[29] J.M. Beck, W.J. Ma, R. Kiani, T. Hanks, A.K. Churchland, J. Roitman, M. N. Shadlen, P.E. Latham, A. Pouget, Probabilistic population codes for bayesian decision making, Neuron 60 (2008) 1142–1152, https://doi.org/10.1016/j.neuron.2008.09.021.
[30] W.J. Ma, J.M. Beck, P.E. Latham, A. Pouget, Bayesian inference with probabilistic population codes, Nat. Neurosci. 9 (2006) 1432–1438, https://doi.org/10.1038/nn1790.
[31] D.D. Garrett, N. Kovacevic, A.R. McIntosh, C.L. Grady, The importance of being variable, J. Neurosci. 31 (2011) 4496, https://doi.org/10.1523/JNEUROSCI.5641-10.2011.
[32] C.L. Grady, D.D. Garrett, Understanding variability in the BOLD signal and why it matters for aging, Brain Imaging Behav. 8 (2014) 274–283, https://doi.org/10.1007/s11682-013-9253-0.

[33] J.S. Nomi, T.S. Bolt, C.E.C. Ezie, L.Q. Uddin, A.S. Heller, Moment-to-moment BOLD signal variability reflects regional changes in neural flexibility across the lifespan, J. Neurosci. 37 (2017) 5539, https://doi.org/10.1523/JNEUROSCI.3408-16.2017.

[34] V. Kebets, P. Favre, J. Houenou, M. Polosan, N. Perroud, J.-M. Aubry, D. Van De Ville, C. Piguet, Fronto-limbic neural variability as a transdiagnostic correlate of emotion dysregulation, Transl. Psychiatry 11 (2021) 545, https://doi.org/10.1038/s41398-021-01666-3.

[35] L. Li, Y. Wang, L. Ye, W. Chen, X. Huang, Q. Cui, Z. He, D. Liu, H. Chen, Altered brain signal variability in patients with generalized anxiety disorder, Front. Psychiatry 10 (2019) 84, https://doi.org/10.3389/fpsyt.2019.00084.

[36] K.N.T. Månsson, L. Waschke, A. Manzouri, T. Furmark, H. Fischer, D.D. Garrett, Moment-to-moment brain signal variability reliably predicts psychiatric treatment outcome, Biol. Psychiatry (2021), https://doi.org/10.1016/j.biopsych.2021.09.026.

[37] M. Martino, P. Magioncalda, Z. Huang, B. Conio, N. Piaggio, N.W. Duncan, G. Rocchi, A. Escelsior, V. Marozzi, A. Wolff, M. Inglese, M. Amore, G. Northoff, Contrasting variability patterns in the default mode and sensorimotor networks balance in bipolar depression and mania, Proc. Natl. Acad. Sci. U.S.A. 113 (2016) 4824, https://doi.org/10.1073/pnas.1517558113.

[38] J.S. Nomi, E. Schettini, W. Voorhies, T.S. Bolt, A.S. Heller, L.Q. Uddin, Resting-state brain signal variability in prefrontal cortex is associated with ADHD symptom severity in children, Front. Hum. Neurosci. 12 (2018) 90, https://doi.org/10.3389/fnhum.2018.00090.

[39] V. Scarapicchia, E.L. Mazerolle, J.D. Fisk, L.J. Ritchie, J.R. Gawryluk, Resting state BOLD variability in alzheimer's disease: a marker of cognitive decline or cerebrovascular status? Front. Aging Neurosci. 10 (2018) 39, https://doi.org/10.3389/fnagi.2018.00039.

[40] J. Zhang, W. Cheng, Z. Liu, K. Zhang, X. Lei, Y. Yao, B. Becker, Y. Liu, K. M. Kendrick, G. Lu, J. Feng, Neural, electrophysiological and anatomical basis of brain-network variability and its characteristic changes in mental disorders, Brain 139 (2016) 2307–2321, https://doi.org/10.1093/brain/aww143.

[41] C.C. Guo, V.T. Nguyen, M.P. Hyett, G.B. Parker, M.J. Breakspear, Out-of-sync: disrupted neural activity in emotional circuitry during film viewing in melancholic depression, Sci. Rep. 5 (2015) 11605, https://doi.org/10.1038/srep11605.

[42] V. Kebets, J. Houenou, A.-L. Küng, N. Hamdani, M. Leboyer, J.-M. Aubry, A. Dayer, D. Van de Ville, C. Piguet, S133. Resting state bold signal variability correlates with clinical dimensions in euthymic bipolar patients, Biol. Psychiatry 83 (2018) S399.

[43] B. Conio, P. Magioncalda, M. Martino, S. Tumati, L. Capobianco, A. Escelsior, G. Adavastro, D. Russo, M. Amore, M. Inglese, G. Northoff, Opposing patterns of neuronal variability in the sensorimotor network mediate cyclothymic and depressive temperaments, Hum. Brain Mapp. 40 (2019) 1344–1352, https://doi.org/10.1002/hbm.24453.

[44] B.S.C. Wade, S.H. Joshi, T. Pirnia, A.M. Leaver, R.P. Woods, P.M. Thompson, R. Espinoza, K.L. Narr, Random forest classification of depression status based on subcortical brain morphometry following electroconvulsive therapy, in: 2015 IEEE 12th International Symposium on Biomedical Imaging (ISBI), 2015: pp. 92–96. ⟨https://doi.org/10.1109/ISBI.2015.7163824⟩.

[45] R.B. Rutledge, A.M. Chekroud, Q.J. Huys, Machine learning and big data in psychiatry: toward clinical applications, Curr. Opin. Neurobiol. 55 (2019) 152–159, https://doi.org/10.1016/j.conb.2019.02.006.

[46] D. Bzdok, A. Meyer-Lindenberg, Machine learning for precision psychiatry: opportunities and challenges, Biol. Psychiatry Cogn. Neurosci. Neuroimaging 3 (2018) 223–230, https://doi.org/10.1016/j.bpsc.2017.11.007.

[47] M.J. Patel, A. Khalaf, H.J. Aizenstein, Studying depression using imaging and machine learning methods, NeuroImage Clin. 10 (2016) 115–123, https://doi.org/10.1016/j.nicl.2015.11.003.

[48] N. Haslam, A.T. Beck, Categorization of major depression in an outpatient sample, J. Nerv. Ment. Dis. 181 (1993) 725–731, https://doi.org/10.1097/00005053-199312000-00003.

[49] S.N. Gosnell, J.C. Fowler, R. Salas, Classifying suicidal behavior with resting-state functional connectivity and structural neuroimaging, Acta Psychiatr. Scand. 140 (2019) 20–29, https://doi.org/10.1111/acps.13029.

[50] W. Mumtaz, S.S.A. Ali, M.A.M. Yasin, A.S. Malik, A machine learning framework involving EEG-based functional connectivity to diagnose major depressive disorder (MDD, Med. Biol. Eng. Comput. 56 (2018) 233–246, https://doi.org/10.1007/s11517-017-1685-z.

[51] M.J. Patel, C. Andreescu, J.C. Price, K.L. Edelman, C.F. Reynolds III, H. J. Aizenstein, Machine learning approaches for integrating clinical and imaging features in late-life depression classification and response prediction, Int. J. Geriatr. Psychiatry 30 (2015) 1056–1067, https://doi.org/10.1002/gps.4262.

[52] M.D. Sacchet, G. Prasad, L.C. Foland-Ross, P.M. Thompson, I.H. Gotlib, Support vector machine classification of major depressive disorder using diffusion-weighted neuroimaging and graph theory, Front. Psychiatry 6 (2015) https://www.frontiersin.org/article/10.3389/fpsyt.2015.00021.

[53] Y. Shimizu, J. Yoshimoto, S. Toki, M. Takamura, S. Yoshimura, Y. Okamoto, S. Yamawaki, K. Doya, Toward probabilistic diagnosis and understanding of depression based on functional MRI data analysis with logistic group LASSO, PLoS One 10 (2015), e0123524, https://doi.org/10.1371/journal.pone.0123524.

[54] L.-L. Zeng, H. Shen, L. Liu, L. Wang, B. Li, P. Fang, Z. Zhou, Y. Li, D. Hu, Identifying major depression using whole-brain functional connectivity: a multivariate pattern analysis, Brain 135 (2012) 1498–1507, https://doi.org/10.1093/brain/aws059.

[55] L.-L. Zeng, H. Shen, L. Liu, D. Hu, Unsupervised classification of major depression using functional connectivity MRI, Hum. Brain Mapp. 35 (2014) 1630–1641, https://doi.org/10.1002/hbm.22278.

[56] G. Gaut, B. Turner, Z.-L. Lu, X. Li, W.A. Cunningham, M. Steyvers, Predicting task and subject differences with functional connectivity and blood-oxygen-level-dependent variability, Brain Connect. 9 (2019) 451–463, https://doi.org/10.1089/brain.2018.0632.

[57] A.E. Gaffey, E.C. Walsh, C.O. Ladd, R.M. Hoks, H.C. Abercrombie, Alterations in systemic and cognitive glucocorticoid sensitivity in depression, Biol. Psychiatry Cogn. Neurosci. Neuroimaging 4 (2019) 310–320, https://doi.org/10.1016/j.bpsc.2018.11.007.

[58] H.C. Abercrombie, C.P. Frost, E.C. Walsh, R.M. Hoks, M.D. Cornejo, M.C. Sampe, A.E. Gaffey, D.T. Plante, C.O. Ladd, R.M. Birn, Neural signaling of cortisol, childhood emotional abuse, and depression-related memory bias, Biol. Psychiatry.: Cogn. Neurosci. Neuroimaging 3 (2018) 274–284, https://doi.org/10.1016/j.bpsc.2017.11.005.

[59] C.N. Rivera-Bonet, R.M. Birn, C.O. Ladd, M.E. Meyerand, H.C. Abercrombie, Cortisol effects on brain functional connectivity during emotion processing in women with depression, J. Affect. Disord. 287 (2021) 247–254, https://doi.org/10.1016/j.jad.2021.03.034.

[60] M.B. First, R.L. Spitzer, G. Miriam, B.W. Janet, Structured Clinical Interview for DSM-IV-TR Axis I Disorders, Research Version, Patient Edition., Biometrics Research, New York State Psychiatric Institute, New York, 2002.

[61] A.T. Beck, R.A. Steer, G.K. Brown, Beck Depression Inventory-II, Psychological Corporation, San Antonio, TX, 1996.

[62] R.W. Cox, AFNI: software for analysis and visualization of functional magnetic resonance neuroimages, Comput. Biomed. Res. 29 (1996) 162–173, https://doi.org/10.1006/cbmr.1996.0014.

[63] G. Salimi-Khorshidi, G. Douaud, C.F. Beckmann, M.F. Glasser, L. Griffanti, S. M. Smith, Automatic denoising of functional MRI data: Combining independent component analysis and hierarchical fusion of classifiers, NeuroImage 90 (2014) 449–468, https://doi.org/10.1016/j.neuroimage.2013.11.046.

[64] L. Griffanti, G. Douaud, J. Bijsterbosch, S. Evangelisti, F. Alfaro-Almagro, M. F. Glasser, E.P. Duff, S. Fitzgibbon, R. Westphal, D. Carone, C.F. Beckmann, S. M. Smith, Hand classification of fMRI ICA noise components, NeuroImage 154 (2017) 188–205, https://doi.org/10.1016/j.neuroimage.2016.12.036.

[65] R. Ciric, D.H. Wolf, J.D. Power, D.R. Roalf, G.L. Baum, K. Ruparel, R. T. Shinohara, M.A. Elliott, S.B. Eickhoff, C. Davatzikos, R.C. Gur, R.E. Gur, D. S. Bassett, T.D. Satterthwaite, Benchmarking of participant-level confound regression strategies for the control of motion artifact in studies of functional connectivity, NeuroImage 154 (2017) 174–187, https://doi.org/10.1016/j.neuroimage.2017.03.020.

[66] B. Avants, J.C. Gee, Geodesic estimation for large deformation anatomical shape averaging and interpolation, NeuroImage 23 (2004) S139–S150, https://doi.org/10.1016/j.neuroimage.2004.07.010.

[67] Y. Zhang, M. Brady, S. Smith, Segmentation of brain MR images through a hidden Markov random field model and the expectation-maximization algorithm, IEEE Trans. Med. Imaging 20 (2001) 45–57, https://doi.org/10.1109/42.906424.

[68] R.M. Birn, J.B. Diamond, M.A. Smith, P.A. Bandettini, Separating respiratory-variation-related fluctuations from neuronal-activity-related fluctuations in fMRI, NeuroImage 31 (2006) 1536–1548, https://doi.org/10.1016/j.neuroimage.2006.02.048.

[69] J. Carp, The secret lives of experiments: methods reporting in the fMRI literature, NeuroImage 63 (2012) 289–300, https://doi.org/10.1016/j.neuroimage.2012.07.004.

[70] S.D. Forman, J.D. Cohen, M. Fitzgerald, W.F. Eddy, M.A. Mintun, D.C. Noll, Improved assessment of significant activation in functional magnetic resonance imaging (fMRI): use of a cluster-size threshold, Magn. Reson. Med. 33 (1995) 636–647, https://doi.org/10.1002/mrm.1910330508.

[71] F. Faul, E. Erdfelder, A. Buchner, A.-G. Lang, Statistical power analyses using G*Power 3.1: tests for correlation and regression analyses, Behav. Res. Methods 41 (2009) 1149–1160, https://doi.org/10.3758/BRM.41.4.1149.

[72] L. Breiman, Random forests, Mach. Learn. 45 (2001) 5–32, https://doi.org/10.1023/A:1010933404324.

[73] L. Breiman, A. Cutler, Random forests., 2005. ⟨https://www.stat.berkeley.edu/~breiman/RandomForests/cc_home.htm⟩.

[74] A.R. Laird, S.B. Eickhoff, K. Li, D.A. Robin, D.C. Glahn, P.T. Fox, Investigating the functional heterogeneity of the default mode network using coordinate-based meta-analytic modeling, J. Neurosci. 29 (2009) 14496, https://doi.org/10.1523/JNEUROSCI.4004-09.2009.

[75] W.W. Seeley, V. Menon, A.F. Schatzberg, J. Keller, G.H. Glover, H. Kenna, A. L. Reiss, M.D. Greicius, Dissociable intrinsic connectivity networks for salience processing and executive control, J. Neurosci. 27 (2007) 2349, https://doi.org/10.1523/JNEUROSCI.5587-06.2007.

[76] A. Liaw, M. Wiener, Classification and regression by randomForest, R News. 2, 2002, 18–22.

[77] P. Probst, M.N. Wright, A.-L. Boulesteix, Hyperparameters and tuning strategies for random forest, WIREs Data Min. Knowl. Discov. 9 (2019), e1301, https://doi.org/10.1002/widm.1301.

[78] J.D. Schmahmann, J.C. Sherman, The cerebellar cognitive affective syndrome, Brain 121 (1998) 561–579, https://doi.org/10.1093/brain/121.4.561.

[79] J.C. Soares, J.J. Mann, The anatomy of mood disorders—review of structural neuroimaging studies, Biol. Psychiatry 41 (1997) 86–106, https://doi.org/10.1016/S0006-3223(96)00006-6.

[80] M.S. Depping, M.M. Schmitgen, K.M. Kubera, R.C. Wolf, Cerebellar contributions to major depression, Front. Psychiatry 9 (2018) https://www.frontiersin.org/article/10.3389/fpsyt.2018.00634.
[81] M.S. Depping, N.D. Wolf, N. Vasic, Z. Sosic-Vasic, M.M. Schmitgen, F. Sambataro, R.C. Wolf, Aberrant resting-state cerebellar blood flow in major depression, J. Affect. Disord. 226 (2018) 227–231, https://doi.org/10.1016/j.jad.2017.09.028.
[82] L. Liu, L.-L. Zeng, Y. Li, Q. Ma, B. Li, H. Shen, D. Hu, Altered cerebellar functional connectivity with intrinsic connectivity networks in adults with major depressive disorder, PLoS One 7 (2012), e39516, https://doi.org/10.1371/journal.pone.0039516.
[83] W. Guo, F. Liu, Z. Xue, K. Gao, Z. Liu, C. Xiao, H. Chen, J. Zhao, Abnormal resting-state cerebellar–cerebral functional connectivity in treatment-resistant depression and treatment sensitive depression, Prog. Neuro Psychopharmacol. Biol. Psychiatry 44 (2013) 51–57, https://doi.org/10.1016/j.pnpbp.2013.01.010.
[84] Y. Song, S. Sun, X. Song, N. Mao, B. Wang, BOLD-fMRI study on the basic activity of the brain in major disorder depression and their first-degree relatives, J. Pract. Radiol. 33 (2017) 653–657.
[85] C. Yang, A. Zhang, A. Jia, J.X. Ma, N. Sun, Y. Wang, X. Li, Z. Liu, S. Liu, Y. Xu, K. Zhang, Identify abnormalities in resting-state brain function between first-episode, drug-naive major depressive disorder and remitted individuals: a 3-year retrospective study, NeuroReport 29 (2018) 907–916, https://doi.org/10.1097/WNR.0000000000001054.
[86] T. Yamamura, Y. Okamoto, G. Okada, Y. Takaishi, M. Takamura, A. Mantani, A. Kurata, Y. Otagaki, H. Yamashita, S. Yamawaki, Association of thalamic hyperactivity with treatment-resistant depression and poor response in early treatment for major depression: a resting-state fMRI study using fractional amplitude of low-frequency fluctuations, Transl. Psychiatry 6 (2016), https://doi.org/10.1038/tp.2016.18.
[87] J. Gong, J. Wang, S. Qiu, P. Chen, Z. Luo, J. Wang, L. Huang, Y. Wang, Common and distinct patterns of intrinsic brain activity alterations in major depression and bipolar disorder: voxel-based meta-analysis, Transl. Psychiatry 10 (2020) 353, https://doi.org/10.1038/s41398-020-01036-5.
[88] R.L. Buckner, J.R. Andrews-Hanna, D.L. Schacter, The brain's default network, Ann. N.Y. Acad. Sci. 1124 (2008) 1–38, https://doi.org/10.1196/annals.1440.011.
[89] T. Engelen, T.A. de Graaf, A.T. Sack, B. de Gelder, A causal role for inferior parietal lobule in emotion body perception, Cortex 73 (2015) 195–202, https://doi.org/10.1016/j.cortex.2015.08.013.
[90] M. Iacoboni, Neural mechanisms of imitation, Curr. Opin. Neurobiol. 15 (2005) 632–637, https://doi.org/10.1016/j.conb.2005.10.010.
[91] C. Keysers, V. Gazzola, Expanding the mirror: vicarious activity for actions, emotions, and sensations, Curr. Opin. Neurobiol. 19 (2009) 666–671, https://doi.org/10.1016/j.conb.2009.10.006.
[92] M.L. Seghier, The angular gyrus: multiple functions and multiple subdivisions, Neuroscientist 19 (2013) 43–61, https://doi.org/10.1177/1073858412440596.
[93] S. Kajimura, T. Kochiyama, R. Nakai, N. Abe, M. Nomura, Causal relationship between effective connectivity within the default mode network and mind-wandering regulation and facilitation, NeuroImage 133 (2016) 21–30, https://doi.org/10.1016/j.neuroimage.2016.03.009.
[94] J. Wang, Y. Yang, L. Fan, J. Xu, C. Li, Y. Liu, P.T. Fox, S.B. Eickhoff, C. Yu, T. Jiang, Convergent functional architecture of the superior parietal lobule unraveled with multimodal neuroimaging approaches, Hum. Brain Mapp. 36 (2015) 238–257, https://doi.org/10.1002/hbm.22626.
[95] L. Wang, W. Dai, Y. Su, G. Wang, Y. Tan, Z. Jin, Y. Zeng, X. Yu, W. Chen, X. Wang, T. Si, Amplitude of low-frequency oscillations in first-episode, treatment-naive patients with major depressive disorder: a resting-state functional MRI study, PLoS One 7 (2012), e48658, https://doi.org/10.1371/journal.pone.0048658.
[96] H.-L. Yu, W.-B. Liu, T. Wang, P.-Y. Huang, L.-Y. Jie, J.-Z. Sun, C. Wang, W. Qian, M. Xuan, Q.-Q. Gu, H. Liu, F.-L. Zhang, M.-M. Zhang, Difference in resting-state fractional amplitude of low-frequency fluctuation between bipolar depression and unipolar depression patients, Eur. Rev. Med Pharmacol. Sci. 21 (2017) 1541–1550.
[97] X. Di, E.H. Kim, C.-C. Huang, C.-P. Lin, B. Biswal, The influence of the amplitude of low-frequency fluctuations on resting-state functional connectivity, Front. Hum. Neurosci. 7 (2013) https://www.frontiersin.org/article/10.3389/fnhum.2013.00118.
[98] Z. Fu, Y. Tu, X. Di, B.B. Biswal, V.D. Calhoun, Z. Zhang, Associations between functional connectivity dynamics and BOLD dynamics are heterogeneous across brain networks, Front. Hum. Neurosci. 11 (2017) https://www.frontiersin.org/article/10.3389/fnhum.2017.00593.
[99] W. Guo, F. Liu, Z. Xue, X. Xu, R. Wu, C. Ma, S.C. Wooderson, C. Tan, X. Sun, J. Chen, Z. Liu, C. Xiao, H. Chen, J. Zhao, Alterations of the amplitude of low-frequency fluctuations in treatment-resistant and treatment-response depression: a resting-state fMRI study, Prog. Neuro Psychopharmacol. Biol. Psychiatry 37 (2012) 153–160, https://doi.org/10.1016/j.pnpbp.2012.01.011.
[100] L. Liu, L.-L. Zeng, Y. Li, Q. Ma, B. Li, H. Shen, D. Hu, Altered cerebellar functional connectivity with intrinsic connectivity networks in adults with major depressive disorder, PLoS One 7 (2012), e39516, https://doi.org/10.1371/journal.pone.0039516.
[101] X. Wei, H. Shen, J. Ren, W. Liu, R. Yang, J. Liu, H. Wu, X. Xu, L. Lai, J. Hu, X. Pan, X. Jiang, Alteration of spontaneous neuronal activity in young adults with non-clinical depressive symptoms, Psychiatry Res. Neuroimaging 233 (2015) 36–42, https://doi.org/10.1016/j.pscychresns.2015.04.008.
[102] L. Schmaal, E. Pozzi, T.C. Ho, L.S. van Velzen, I.M. Veer, N. Opel, E.J.W. Van Someren, L.K.M. Han, L. Aftanas, A. Aleman, B.T. Baune, K. Berger, T.F. Blanken, L. Capitão, B. Couvy-Duchesne, K.R. Cullen, U. Dannlowski, C. Davey, T. Erwin-Grabner, J. Evans, T. Frodl, C.H.Y. Fu, B. Godlewska, I.H. Gotlib, R. Goya-Maldonado, H.J. Grabe, N.A. Groenewold, D. Grotegerd, O. Gruber, B.A. Gutman, G.B. Hall, B.J. Harrison, S.N. Hatton, M. Hermesdorf, I.B. Hickie, E. Hilland, B. Irungu, R. Jonassen, S. Kelly, T. Kircher, B. Klimes-Dougan, A. Krug, N. I. Landrø, J. Lagopoulos, J. Leerssen, M. Li, D.E.J. Linden, F.P. MacMaster, A. M. McIntosh, D.M.A. Mehler, I. Nenadić, B.W.J.H. Penninx, M.J. Portella, L. Reneman, M.E. Rentería, M.D. Sacchet, P.G. Sämann, A. Schrantee, K. Sim, J. C. Soares, D.J. Stein, L. Tozzi, N.J.A. van Der Wee, M.-J. van Tol, R. Vermeiren, Y. Vives-Gilabert, H. Walter, M. Walter, H.C. Whalley, K. Wittfeld, S. Whittle, M. J. Wright, T.T. Yang, C. Zarate, S.I. Thomopoulos, N. Jahanshad, P.M. Thompson, D.J. Veltman, ENIGMA MDD: seven years of global neuroimaging studies of major depression through worldwide data sharing, Transl. Psychiatry 10 (2020) 172, https://doi.org/10.1038/s41398-020-0842-6.
[103] G. Li, Y. Liu, Y. Zheng, D. Li, X. Liang, Y. Chen, Y. Cui, P.-T. Yap, S. Qiu, H. Zhang, D. Shen, Large-scale dynamic causal modeling of major depressive disorder based on resting-state functional magnetic resonance imaging, Hum. Brain Mapp. 41 (2020) 865–881, https://doi.org/10.1002/hbm.24845.
[104] Y. Long, H. Cao, C. Yan, X. Chen, L. Li, F.X. Castellanos, T. Bai, Q. Bo, G. Chen, N. Chen, W. Chen, C. Cheng, Y. Cheng, X. Cui, J. Duan, Y. Fang, Q. Gong, W. Guo, Z. Hou, L. Hu, L. Kuang, F. Li, K. Li, T. Li, Y. Liu, Q. Luo, H. Meng, D. Peng, H. Qiu, J. Qiu, Y. Shen, Y. Shi, T. Si, C. Wang, F. Wang, K. Wang, L. Wang, X. Wang, Y. Wang, X. Wu, X. Wu, C. Xie, G. Xie, H. Xie, P. Xie, X. Xu, H. Yang, J. Yang, J. Yao, S. Yao, Y. Yin, Y. Yuan, A. Zhang, H. Zhang, K. Zhang, L. Zhang, Z. Zhang, R. Zhou, Y. Zhou, J. Zhu, C. Zou, Y. Zang, J. Zhao, C. Kin-yuen Chan, W. Pu, Z. Liu, Altered resting-state dynamic functional brain networks in major depressive disorder: Findings from the REST-meta-MDD consortium, NeuroImage Clin. 26 (2020), 102163, https://doi.org/10.1016/j.nicl.2020.102163.
[105] Q. Li, Y. Zhao, Z. Chen, J. Long, J. Dai, X. Huang, S. Lui, J. Radua, E. Vieta, G. J. Kemp, J.A. Sweeney, F. Li, Q. Gong, Meta-analysis of cortical thickness abnormalities in medication-free patients with major depressive disorder, Neuropsychopharmacology 45 (2020) 703–712, https://doi.org/10.1038/s41386-019-0563-9.
[106] C.-G. Yan, X. Chen, L. Li, X. Castellanos Francisco, T.-J. Bai, Q.-J. Bo, J. Cao, G.-M. Chen, N.-X. Chen, W. Chen, C. Cheng, Y.-Q. Cheng, X.-L. Cui, J. Duan, Y.-R. Fang, Q.-Y. Gong, W.-B. Guo, Z.-H. Hou, L. Hu, L. Kuang, F. Li, K.-M. Li, T. Li, Y.-S. Liu, Z.-N. Liu, Y.-C. Long, Q.-H. Luo, H.-Q. Meng, D.-H. Peng, H.-T. Qiu, J. Qiu, Y.-D. Shen, Y.-S. Shi, C.-Y. Wang, F. Wang, K. Wang, L. Wang, X. Wang, Y. Wang, X.-P. Wu, X.-R. Wu, C.-M. Xie, G.-R. Xie, H.-Y. Xie, P. Xie, X.-F. Xu, H. Yang, J. Yang, J.-S. Yao, S.-Q. Yao, Y.-Y. Yin, Y.-G. Yuan, A.-X. Zhang, H. Zhang, K.-R. Zhang, L. Zhang, Z.-J. Zhang, R.-B. Zhou, Y.-T. Zhou, J.-J. Zhu, C.-J. Zou, T.-M. Si, X.-N. Zuo, J.-P. Zhao, Y.-F. Zang, Reduced default mode network functional connectivity in patients with recurrent major depressive disorder, Proc. Natl. Acad. Sci. 116 (2019) 9078–9083, https://doi.org/10.1073/pnas.1900390116.
[107] Z. Cui, G. Gong, The effect of machine learning regression algorithms and sample size on individualized behavioral prediction with functional connectivity features, NeuroImage 178 (2018) 622–637, https://doi.org/10.1016/j.neuroimage.2018.06.001.
[108] A.N. Nielsen, D.M. Barch, S.E. Petersen, B.L. Schlaggar, D.J. Greene, Machine learning with neuroimaging: evaluating its applications in psychiatry, Biol. Psychiatry Cogn. Neurosci. Neuroimaging 5 (2020) 791–798, https://doi.org/10.1016/j.bpsc.2019.11.007.
[109] T. van der Ploeg, P.C. Austin, E.W. Steyerberg, Modern modelling techniques are data hungry: a simulation study for predicting dichotomous endpoints, BMC Med. Res. Methodol. 14 (2014) 137, https://doi.org/10.1186/1471-2288-14-137.
[110] R. Zhang, G.S. Kranz, W. Zou, Y. Deng, X. Huang, K. Lin, T.M.C. Lee, Rumination network dysfunction in major depression: a brain connectome study, Prog. Neuro Psychopharmacol. Biol. Psychiatry 98 (2020), 109819, https://doi.org/10.1016/j.pnpbp.2019.109819.
[111] S. Marek, B. Tervo-Clemmens, F.J. Calabro, D.F. Montez, B.P. Kay, A.S. Hatoum, M.R. Donohue, W. Foran, R.L. Miller, T.J. Hendrickson, S.M. Malone, S. Kandala, E. Feczko, O. Miranda-Dominguez, A.M. Graham, E.A. Earl, A.J. Perrone, M. Cordova, O. Doyle, L.A. Moore, G.M. Conan, J. Uriarte, K. Snider, B.J. Lynch, J.C. Wilgenbusch, T. Pengo, A. Tam, J. Chen, D.J. Newbold, A. Zheng, N. A. Seider, A.N. Van, A. Metoki, R.J. Chauvin, T.O. Laumann, D.J. Greene, S. E. Petersen, H. Garavan, W.K. Thompson, T.E. Nichols, B.T.T. Yeo, D.M. Barch, B. Luna, D.A. Fair, N.U.F. Dosenbach, Reproducible brain-wide association studies require thousands of individuals, Nature 603 (2022) 654–660, https://doi.org/10.1038/s41586-022-04492-9.
[112] X.-N. Zuo, T. Xu, M.P. Milham, Harnessing reliability for neuroscience research, Nat. Hum. Behav. 3 (2019) 768–771, https://doi.org/10.1038/s41562-019-0655-x.
[113] X.-N. Zuo, A. Di Martino, C. Kelly, Z.E. Shehzad, D.G. Gee, D.F. Klein, F. X. Castellanos, B.B. Biswal, M.P. Milham, The oscillating brain: complex and reliable, NeuroImage 49 (2010) 1432–1445, https://doi.org/10.1016/j.neuroimage.2009.09.037.
[114] D.D. Garrett, N. Kovacevic, A.R. McIntosh, C.L. Grady, The modulation of BOLD variability between cognitive states varies by age and processing speed, Cereb. Cortex 23 (2013) 684–693, https://doi.org/10.1093/cercor/bhs055.
[115] K.N.T. Månsson, L. Waschke, A. Manzouri, T. Furmark, H. Fischer, D.D. Garrett, Moment-to-moment brain signal variability reliably predicts psychiatric treatment outcome, Biol. Psychiatry 91 (2022) 658–666, https://doi.org/10.1016/j.biopsych.2021.09.026.
[116] D.J.L.G. Schutter, D. Martin Laman, J. van Honk, A.C. Vergouwen, G. Frank Koerselman, Partial clinical response to 2 weeks of 2 Hz repetitive transcranial

magnetic stimulation to the right parietal cortex in depression, Int. J. Neuropsychopharmacol. 12 (2009) 643–650, https://doi.org/10.1017/S1461145708009553.

[117] D.J.L.G. Schutter, J. van Honk, A.A.L. d'Alfonso, J.S. Peper, J. Panksepp, High frequency repetitive transcranial magnetic over the medial cerebellum induces a shift in the prefrontal electroencephalography gamma spectrum: a pilot study in humans, Neurosci. Lett. 336 (2003) 73–76, https://doi.org/10.1016/S0304-3940(02)01077-7.

[118] D.J.L.G. Schutter, J. van Honk, A framework for targeting alternative brain regions with repetitive transcranial magnetic stimulation in the treatment of depression, J. Psychiatry Neurosci. 30 (2005) 91–97.

[119] J. van Honk, D.J.L.G. Schutter, P. Putman, E.H.F. de Haan, A.A.L. d'Alfonso, Reductions in phenomenological, physiological and attentional indices of depressive mood after 2 Hz rTMS over the right parietal cortex in healthy human subjects, Psychiatry Res. 120 (2003) 95–101, https://doi.org/10.1016/S0165-1781(03)00114-8.

[120] N.K. Rytwinski, M.D. Scur, N.C. Feeny, E.A. Youngstrom, The co-occurrence of major depressive disorder among individuals with posttraumatic stress disorder: a meta-analysis, J. Trauma. Stress 26 (2013) 299–309, https://doi.org/10.1002/jts.21814.